

# The feature enhancement method of artistic images based on histogram equalization and bilateral filtering

Wenjing Zhang <sup>Corresp. 1</sup>

<sup>1</sup> Art School, Zhengzhou University of Technology, Zhengzhou 450064, China

Corresponding Author: Wenjing Zhang  
Email address: meilandusci@163.com

To improve the rendering effect of artistic images, a method enhancing features of artistic images is proposed based on histogram equalization and bilateral filtering in the article. Firstly, artistic images are divided into both high and low-frequency representations, and the multi-step enhancement processing level is delimited by multi-band decomposition. Secondly, the noise in the image is removed by bilateral filtering. Then, the grey-level histogram of the image is modified by using the histogram equalization. Finally, the features of the artistic image are enhanced by global tone mapping after histogram equalization processing is conducted. Then, the image is sharpened to improve the enhancement effect further. The experiments show that the features of the color and edge details turn out to be more vivid and clearer after the proposed method is implemented. The structural similarity (SSIM) measure of the image increases to 0.973, and the average gradient gets close to 0.8, which shows that the proposed method is effective.

# The feature enhancement method of artistic images based on histogram equalization and bilateral filtering

Wenjing Zhang

Art School, Zhengzhou University of Science and Technology, Zhengzhou  
450064, China

Corresponding author: Wenjing Zhang (e-mail:meilandusci@163.com).

**Abstract:** To improve the rendering effect of artistic images, a method enhancing features of artistic images is proposed based on histogram equalization and bilateral filtering in the article. Firstly, artistic images are divided into both high and low-frequency representations, and the multi-step enhancement processing level is delimited by multi-band decomposition. Secondly, the noise in the image is removed by bilateral filtering. Then, the grey-level histogram of the image is modified by using the histogram equalization. Finally, the features of the artistic image are enhanced by global tone mapping after histogram equalization processing is conducted. Then, the image is sharpened to improve the enhancement effect further. The experiments show that the features of the color and edge details turn out to be more vivid and clearer after the proposed method is implemented. The structural similarity (SSIM) measure of the image increases to 0.973, and the average gradient gets close to 0.8, which shows that the proposed method is effective.

**Keywords:** Artistic images; Feature enhancement processing; Histogram equalization processing; Bilateral filtering; Full-color sharpening; digital art enhancement

## 1 Introduction

An artistic image is a graphical kind of symbol produced by artistic means, which is formed by the internal logic system of complex visual graphics. Its elements are mainly composed of modeling points, lines, surfaces, bodies, blocks, colors, textures, etc.. It is relatively different from the original graphics in nature [1]. This image is a visual form created by certain requirements and modeling rules. Distinct from practical images, artistic images follow more subjective and aesthetic expression with more artistic and creative forms [2].

The main reason for implementing feature enhancement on artistic images is to highlight the effective interesting features to be processed while diluting or removing unwanted information. To enhance the features of the image, its visual effect and clarity can be improved, and the visual perception and aesthetic needs of human beings can be better met [3-4]. At the same time, feature enhancement can also provide more representative information for subsequent image analysis and processing and thus improve the accuracy and efficiency of image processing.

For example, a method enhancing image features is proposed based on a convolutional network (CNN) model, which uses an image color model and denoising autoencoder to complete

39 the pre-processing of low-illumination images [5]. Then, the image mapping function is designed  
40 by the piecewise transformation method, and the objective function of the image enhancement is  
41 obtained. Finally, the CNN model and the corresponding loss function are constructed to complete  
42 the image feature enhancement process. An image enhancement method is proposed by combining  
43 feature fusion and physical correction [6]. Self-building blocks are used to replace the feature  
44 fusion network of the encoder and decoder structure of the convolutional layer to correct the color  
45 bias of the image. The improved feature fusion module in the network reduces the damage of the  
46 full connection layer to the image spatial structure, thus protecting the spatial features, and  
47 reducing the number of parameters of the module. Then, the improved attention module is used to  
48 extract texture details and protect background information through parallel pooling computations.  
49 Finally, the multi-color model correction module is employed to correct the relationship between  
50 pixels to further reduce color biases and improve contrast and brightness features. An image  
51 enhancement method is proposed based on multi-level feature fusion that utilizes multiscale  
52 sampling to construct a U-shaped network and introduces multiple attention mechanisms to multi-  
53 thread image flow. The feature vectors of each branch interact across channels to cooperatively  
54 and gradually suppress redundant information. Then, the feature fusion module is employed to  
55 enhance the perception of low-scale texture details and multi-level features, respectively. Finally,  
56 a loss function composed of peak signal-to-noise ratio and structural similarity (SSIM) index is  
57 designed to guide the network to learn the mapping relationship between images from shallow to  
58 deep structures, thus speeding up the convergence of the model and helping improve the model  
59 performance and image enhancement, respectively.

60 However, it is found that SSIM and average gradient of artistic images become low after  
61 processing when the conventional algorithms and the enhancement results are not ideal in practical  
62 applications. To resolve this problem, a new feature enhancement method for artistic images is  
63 designed based on histogram equalization and bilateral filtering. The proposed method is expressed  
64 as follows:

65 Firstly, the form of multi-stage processing is adopted to delimit the multi-stage enhancement  
66 processing level of the image by multi-band decomposition based on dividing the high and low-  
67 frequency representations of an artistic image. To fuse different scales of the image, the structure  
68 information and texture features of the image can be described better, which provides more  
69 powerful support for the subsequent feature enhancement processing. Secondly, the artistic image  
70 is denoised by bilateral filtering. Then, the histogram equalization method is employed to correct  
71 the gray level histogram of the image, so that the pixel intensity distribution of the image becomes  
72 more uniform and the contrast of the image is improved in the end. Finally, the features of the  
73 artistic image are enhanced by global tone mapping. On this basis, the image is sharpened to  
74 highlight the feature edges and details to further improve the enhancement effect after histogram  
75 equalization processing is run.

76 *The rest of the article is outlined as follows: Section 2 presents the proposed method. Section*  
77 *3 is allocated to the experiment and the analysis of the results. Section 4 presents the conclusion.*

78 2 The design of a method used for enhancing the features of the artistic image

79 2.1 High and low-frequency divisions of an artistic image and the level demarcation of the

80 multi-level enhancement processing

81 Based on dividing the high and low-frequency representations of artistic images, this study  
82 adopts the form of multi-stage processing and delimits the multi-stage enhancement processing  
83 level by multi-band decomposition.

84 Usually, it is necessary to divide the high-frequency and low-frequency parts of the image  
85 before processing an artistic image. The high-frequency part mainly contains the details of the  
86 image, such as edge, texture, etc. The low-frequency part generally includes the structural  
87 information of the image, such as contour, shape, etc. Each frequency band corresponds to an  
88 enhanced processing level. Each band or level can be enhanced to highlight the details of that band  
89 or level [8-9].

90 Based on the processing requirements of the actual artistic image, the current transfer function  
91 is measured and calculated, and the best control is generally found between 0.35 and 0.66. Then,  
92 according to the change in the transfer function of the ideal low-pass filter, the cutoff frequency is  
93 measured and calculated in Eq. (1)

$$94 \quad r = t^2 - \sum_{B=1}^{\infty} \omega B + \gamma(1) \quad (1)$$

95 where  $r$  represents the cut-off frequency;  $t$  stands for lossless frequency;  $\omega$  represents  
96 directional high and low frequencies;  $B$  indicates the calibration of the covered area;  $\gamma$  means the  
97 converted mean. When combined with the current measurements, the cutoff frequency is  
98 calculated [10]. On this basis, the image is divided according to the brightness, contrast, color, and  
99 other features, and the multi-level enhancement processing level is designed. The content of the  
100 specific division is shown in Figure 1.

101  
102 Figure 1 A diagram used for multilevel enhancement processing of an artistic image using a  
103 hierarchy classification diagram.

104  
105 When combined with Figure 1, the division of multi-level enhancement processing levels is  
106 realized. The hierarchical delineation of multi-level enhanced processing is to construct multiscale  
107 image representation. To process an image, multiscale analysis is an important method, which can  
108 extract feature information at different scales by processing images at different scales [11-12]. The  
109 image can be divided into several different scales and each scale can be enhanced to obtain a  
110 multiscale image representation.

111 The structure information and texture features of the image can be better described by fusing  
112 the different scales of the image, which provides more powerful support for the subsequent feature  
113 enhancement processing.

## 114 2.2 Bilateral filtering processing of the artistic image

115 *In the above process, the visual quality of artistic images can be improved and the artistic  
116 effect can be enhanced through the division of high and low frequencies and the demarcation of  
117 multi-level enhancement processing levels. On this basis, the denoising of artistic images is  
118 realized by employing bilateral filter processing.*

119 *Bilateral filtering is a kind of filter that can retain edge information and denoise at the same*

120 *time. The reason is that the denoising effect can be achieved with the filter composed of two*  
 121 *functions and the filter coefficient is determined by the geometric space distance and the pixel*  
 122 *difference, respectively [13-14]. The two-sided filter has one more Gaussian variance than the*  
 123 *Gaussian filter, which is a Gaussian filter function based on spatial distribution, so the pixels far*  
 124 *away from the edge will not have a greater impact on the edge pixels to avoid the edge blur [15].*

125 *The bilateral filtering is defined in Eq. (2):*

$$126 \quad F_I = \frac{\sum_{i,j=-w}^w (G_{\sigma_1}(x,y) \times G_{\sigma_2}(x,y) \times I(x,y))}{\sum_{i,j=-w}^w G_{\sigma_1}(x,y) \times G_{\sigma_2}(x,y)} \quad (2)$$

127 *where  $I$  represents the artistic image to be processed;  $F_I$  represents the filtered image, and*  
 128  *$G_{\sigma_1}(x,y)$  represents the Gaussian kernel function, representing the spatial similarity of points with*  
 129  *$(x,y)$  as the center and  $w$  as the radius;  $\sigma_1$  represents the variance parameter;  $G_{\sigma_2}(x,y)$  represents*  
 130 *the pixel similarity of points with  $(x,y)$  as the center and  $w$  as the radius;  $\sigma_2$  represents the variance*  
 131 *parameter.*

132 *The gray value  $h_I$  of the artistic image after bilateral filtering is expressed in Eq. (3):*

$$133 \quad h_I = \frac{\sum_{(x,y) \in n} w_d(x,y) w_h(x,y) \text{gray}(x,y)}{\sum w_d(x,y) w_h(x,y)} \quad (3)$$

134 *where  $w_d(x,y)$  represents the spatial weight of the image;  $w_h(x,y)$  represents the gray*  
 135 *similarity weight of the image;  $\text{gray}(x,y)$  represents the grayscale value of the image at point  $(x,y)$ .*

136 *The expression of the space weight  $w_d(x,y)$  is presented in Eq. (4):*

$$137 \quad w_d(x,y) = \exp\left(-\frac{|o-x|^2 + |k-y|^2}{2\zeta_d^2}\right) \quad (4)$$

138 *where  $\zeta_d$  represents the standard deviation of the space domain;  $(o,k)$  represents any point in*  
 139 *the image other than  $(x,y)$ .*

140 *The similarity weight of the image grayscale  $w_h(x,y)$  is expressed in Eq. (5):*

$$141 \quad w_h(x,y) = \exp\left(-\frac{|\text{gray}(o,k) - \text{gray}(x,y)|^2}{2\zeta_d^2}\right) \quad (5)$$

142 *where  $\zeta_d$  represents the standard deviation of grayscale;  $\text{gray}(o,k)$  denotes the grayscale*  
 143 *value of the image at point  $(o,k)$*

144 *The analysis suggests that the bilateral filtering process is affected by the spatial weight and*  
 145

146 grayscale similarity weight, and there is a linear relationship between the standard deviation of  
 147 the spatial domain and the radius of the filtering window, which will affect the sharpness of the  
 148 artistic image after the bilateral filtering is run [16]. Since more than 95% of the components of  
 149 the Gaussian function are concentrated in the interval  $[-2\zeta_d, 2\zeta_d]$ , the standard deviation  $\zeta_d$  of  
 150 the space domain meets Eq. (6) to ensure the clarity of the image:

$$151 \quad \zeta_d = \frac{aI}{2} \quad (6)$$

152 where  $I$  represents the radius of the filtering window;  $a$  represents the constant, and finally,  
 153 the optimal range of constant changes between 0.80-0.95 through many tests, which can effectively  
 154 prevent image blurring.

155 In addition, the gray standard deviation has a greater impact on the effect of the bilateral  
 156 filtering. Increasing the gray standard deviation can improve the denoising effect, but at the same  
 157 time, the edge details of the image may be lost [17]. A linear relationship exists between gray  
 158 standard deviation and noise variance in the ratio ranging from 2-3. After running many tests,  $\zeta_h$

159  $= 2\zeta_x$  is taken. The noise variance  $\zeta_x$  obtained by the Laplace transform is expressed in Eq.

160 (7):

$$161 \quad \zeta_x = \sqrt{\frac{\pi \sum |\text{gray}(o,k) \times M|}{2^X (X-1)(Y-1)}} \quad (7)$$

162 where  $X$  represents the image width,  $Y$  stands for image height, and  $M$  denotes the discrete  
 163 Laplace transform mask.

164 Thus, the spatial standard deviation and gray standard deviation of the optimized bilateral  
 165 filter are obtained, and the denoising process of the artistic image is completed.

### 166 2.3 Histogram equalization process of the artistic image

167 After image denoising, histogram equalization is used to process the artistic image globally,  
 168 which can enhance the overall contrast of the image and make it more vivid. Histogram  
 169 equalization can make the distribution of pixel intensity more uniform and improve the image  
 170 contrast by correcting the gray-level histogram [18-19]. This method is especially suitable for  
 171 those artistic images with low contrast, which can significantly enhance their detail and color  
 172 levels.

173 Generally, the gray value of each pixel in the image is specified to be between  $[0, 255]$ , and

174 the histogram of the image is represented by a discrete function  $f(h_k) = n_k$ , where  $h_k$  represents

175 the gray value  $n_k$  of any pixel in the image and the number of pixels with gray value  $h_k$  in the image.

176 The gray value of the image can be delineated by the discrete function, and the histogram  
 177 shows the distribution of the image's gray value. In the equalization, the histogram is generally  
 178 normalized and then the gray value is reassigned.

179 Assuming that the infrared image is represented by the tensor  $M \times N$  and the number of image

180 pixels is counted  $MN$ , the normalized histogram can be expressed by Eq. (8):

$$181 \quad p(h_k) = \frac{n_k}{MN} \quad (8)$$

182 where it represents the estimation of the probability that the gray value of the image is  $h_k$ . In  
 183 other words, the normalization method turns all components of the histogram equal to 1 after the  
 184 addition.

185 Based on the above analysis, the processing steps for setting up artistic image histogram  
 186 equalization are as follows:

187 Step 1: The image is divided into two regions. The first region is the low-illuminance region  
 188 with a threshold  $L_L$ , and the second one is the high-illuminance region with a threshold  $L_H$ . Then,  
 189 the image histogram is divided and the sub-histograms of the three images are obtained.

190 Step 2: Establish the probability density function corresponding to the sub-histogram, and  
 191 modify the value of the function;

192 Step 3: According to the correction results, the corrected cumulative distribution function is  
 193 established;

194 Step 4: The image equalization process is completed by combining the modified cumulative  
 195 distribution function with the corrected output function curve of gamma correction.

196 The local features and illumination conditions of artistic images are dynamically adjusted,  
 197 and the threshold of low illumination and high illumination areas can be determined according to  
 198 the key values. The expression for the key value is given in Eq. (9):

$$199 \quad \text{key} = \frac{\bar{L} - L_{\min}}{W_x(L_{\max} - L_{\min})} \quad (9)$$

200 Where  $L_{\min}$  and  $L_{\max}$  represents the lower and upper limits of image brightness, respectively;  
 201  $\bar{L}$  represents the average brightness of the image;  $w$  represents the energy of an image pixel.

202 Based on the key value, the thresholds  $L_L$  and  $L_H$  are determined in Eq. (10):

$$203 \quad \begin{cases} L_L = L_{\max} - \frac{\bar{L}(L_{\max} - L_{\min})}{\text{key}} \\ L_H = L_{\max} - \varepsilon x \text{key}(L_{\max} - L_{\min}) \end{cases} \quad (10)$$

204 where  $\varepsilon$  represents the brightness compensation value.

205 Then, to improve the visibility of the image, the image histogram is divided according to the  
 206 threshold results, and three sub-histograms  $I_1$ ,  $I_2$  and  $I_3$  are obtained, respectively.

207 To avoid edge effects in histogram equalization processing, it is necessary to adjust the  
 208 probability density of sub-histograms to achieve the final probability density function given in Eq.  
 209 (11):

$$210 \quad \rho = \frac{\varepsilon_{\max} \cdot \varepsilon_{\min}}{(L_H - L_L) \cdot \beta} \quad (11)$$

211

212 Where  $g_{max}$  and  $g_{min}$  represents the upper and lower limits of the function values;  $\beta$  indicates  
 213 the adjustment parameters.

214 Since there may be errors in the obtained function value, it needs to be corrected. The  
 215 corrected high-precision probability density function is given in Eq. (12):

$$216 \quad \rho = \frac{\sum_{z=1}^{\max} I^p}{n_j} \quad (12)$$

217 where  $n_j$  represents the number of pixels in the sub-histogram. Since the area with the smaller  
 218 gray level in an artistic image is usually the foreground pixel, the one with the larger gray level is  
 219 usually the background pixel. Therefore, according to the modified probability density function,  
 220 the gamma correction method is used to stretch the pixel level of the sub-histogram of the image,  
 221 to complete the histogram equalization processing of the artistic image.

222 2.4 Enhancing artistic image features based on global tone mapping

223 Based on the artistic image after histogram equalization processing, the features of the artistic  
 224 image are enhanced by employing global tone mapping, which can be regarded as a process of  
 225 gray stretching given in Eq. (13):

$$226 \quad R = \frac{A(x,y)}{V(x,y) + G(x,y) + A(x,y)} \quad (13)$$

227 where  $A(x,y)$  represents the ratio of the pixel value of the image to its mean value;  $V(x,y)$   
 228 represents the local contrast operator, which can stretch the contrast of the image in the local  
 229 neighborhood to highlight the details of the image;  $G(x,y)$  represents the global contrast operator,  
 230 which can enhance the gray level of the darker area and enhance the contrast of the image.

231 Eq. (13) comprehensively considers the global and local contrasts of the artistic image, and  
 232 the distribution range of pixel values in the high-brightness region is reduced in the stretching  
 233 process, while the distribution range of pixel values in the low-brightness region is expanded, thus  
 234 achieving the effect of enhancing image details [20].

235 Eq. (14) delineates how  $A(x,y)$ ,  $V(x,y)$  and  $G(x,y)$  are computed:

$$236 \quad \begin{cases} A(x,y) = \frac{h_1}{h} \\ V(x,y) = \exp\left(\frac{\bar{h}}{h} \left(-\delta \frac{A(x,y)}{h}\right)\right) \\ G(x,y) = \exp\left(\frac{\bar{g}}{g} \left(-\lambda \frac{A(x,y)}{g}\right)\right) \end{cases} \quad (14)$$

237 where  $\bar{h}$  represents the average value of image pixels;  $\delta$  stands for local contrast stretch  
 238 factor;  $\bar{g}$  represents the Gaussian mean of pixel scores in the local neighborhood of the target pixel  
 239 point;  $\lambda$  represents the enhancement coefficient of the global contrast operator.

240 The global contrast of the image decreases with the increase in  $\lambda$  score. When the  $\lambda$   
 241 increases, more details can be seen in the area with a lower gray level of  $\lambda$ , whereas when the  $A$ -  
 242 value decreases, many details of the image cannot be displayed.

243 2.4 Full-color sharpening of artistic images

244 In this study, after the feature enhancement processing of artistic images, the image is further  
 245 sharpened to full-color processing. Sharpening can help highlight the feature edges and details of  
 246 the image, further improving the enhancement effect.

247 Panchromatic sharpening ensures that all color channels of the image are evenly sharpened,  
 248 avoiding color distortion or loss of details. Panchromatic sharpening before feature enhancement  
 249 ensures the quality and consistency of the input image, thus better serving subsequent image  
 250 analysis and processing tasks, respectively. The local correlation coefficient (LCC) is used to  
 251 measure the similarity of spectral features between artistic images and panchromatic images in the  
 252 low-frequency part, and the fourth-order correlation coefficient (FOCC) between the two images  
 253 is calculated, and the fusion coefficient is determined by comparison among them.

254 After the fusion processing of panchromatic image and artistic image, if the LCC score of the  
 255 low-frequency part gets low, it means that the spectral feature similarity score of each pixel  
 256 becomes also low and cannot be replaced. On the contrary, if the local correlation coefficient  
 257 between the artistic images gets large, it indicates that there are a large number of similar spectral  
 258 features in the two artistic images, which can effectively avoid the appearance of image distortion.  
 259 Eq. (15) is used to calculate the local correlation coefficient:

$$260 \quad LCC_s = \frac{K_{a,b}(x,y)}{\sqrt{K_a(x,y)K_b(x,y)}} \quad (15)$$

261  
 262 where  $K_{a,b}(x,y)$  represents the local covariance between any two image blocks  $a$  and  $b$   
 263 centered on pixel point  $(x,y)$ ;  $K_a(i,j)$  and  $K_b(i,j)$  represent the local variances of image blocks  $a$   
 264 and  $b$ .

265 To obtain a more satisfactory panchromatic sharpening effect, the scores of LCCs and FOCC  
 266 are compared to determine whether the high-frequency coefficient needs to be replaced. The four-  
 267 order correlation coefficient evolved based on the correlation coefficient among them, which can  
 268 more accurately measure and describe the SSIM of artistic images. The fourth-order correlation  
 269 coefficient is given by Eq. (16) :

$$270 \quad FOCC_{a,b} = \frac{1}{m \times n} \frac{\sum_{x=1}^X \sum_{y=1}^Y (B(x,y) - \tau_a)^2 (E(x,y) - \tau_b)^2}{\sqrt{\sum_{x=1}^X \sum_{y=1}^Y (B(x,y) - \tau_a)^2 (E(x,y) - \tau_b)^2}} \quad (17)$$

271  
 272 Where  $B(x,y)$  and  $E(x,y)$  represent the image matrix of size  $X \times Y$ ,  $\tau_a$  and  $\tau_b$  represent the  
 273 mean of the matrix.

274 The steps of the panchromatic sharpening of the artistic image are given as follows:

275 Step 1: The artistic image is processed by the Curvelet interpolation method, and NSCT  
 276 transformation is developed to obtain the high and low-frequency coefficient matrix of the artistic  
 277 image, and then a new high and low-frequency coefficient matrix is obtained by NSCT  
 278 transformation.

279 Step 2: For the low-frequency coefficient matrix after the decomposition of the artistic image  
280 and panchromatic image,  $(x,y)$  is selected as the center, the radius is set to 2, and the local  
281 correlation coefficient and fourth-order correlation coefficient of the image block are calculated  
282 by Eqs. (15) and (16), respectively.

283 If the local feature correlation between the target region and the artistic image gets relatively  
284 high, the high-frequency coefficient of the panchromatic image at the point is employed to replace  
285 the high-frequency coefficient of the corresponding point  $(x,y)$  of the artistic image, while  
286 effectively ensuring that there will be no spectral distortion. On the contrary, the high-frequency  
287 coefficient of the artistic image is kept unchanged.

288 Step 3: Expand the NSCT transformation of the low-frequency coefficient and the high-  
289 frequency coefficient of the artistic image after processing, and obtain the artistic image after the  
290 fusion processing is run.

291 Step 4: Expand all the fused images in the RGB color space, and then realize the artistic image  
292 full-color sharpening processing and realize the artistic image feature enhancement processing.

### 293 3 Experiment and the Analysis of the Results

294 To verify the practical application performance of the proposed method used for enhancing  
295 artistic image features based on histogram equalization processing and bilateral filtering, the  
296 following experiments are designed.

#### 297 3.1 Experimental design

298 OpenCV was used as the simulation environment. OpenCV is a widely used open-source  
299 computer vision library that provides rich image processing and computer vision functions and  
300 supports histogram equalization, edge detection, and filter processing of different specifications,  
301 which is suitable for this experiment.

302 The experimental data was gathered from an online platform focused on contemporary art  
303 called the Art Encyclopedia database, which provides a large number of images and related content  
304 of contemporary artworks. In this database, users can search and browse a variety of contemporary  
305 artworks. In this study, 200 artistic images were randomly selected from the Art Encyclopedia  
306 database for the experiment, and the image size was adjusted to  $2500 \times 3000$  with 2 bytes of pixels.

307 To avoid the uniformity of experimental results, the methods in [5] and [6] are employed to  
308 compare performance with the proposed method.

#### 309 3.2 Results

310 Firstly, the two artistic images in Figure 2 are taken as examples to visually compare the  
311 effects of the feature enhancement processing in different methods.

312  
313 Figure 2 The sample image.

314 The processing results of feature enhancement in Figure 2 by different methods are shown in  
315 Figure 3.

316  
317 Figure 3 The results of the feature enhancement processing.

318 To compare Figures 2 and 3, the color features and edge detail features of the image get more  
319 vivid and clear after the proposed method is implemented. However, when the methods in [5] and

320 [6] are applied, the images have different degrees of noise and fading, which cannot effectively  
 321 reflect the characteristics of artistic images.

322 To further verify the image feature enhancement performance of different methods, SSIM,  
 323 and average gradient are employed as indicators.

324 For example, SSIM can be implemented to quantify the retention degree of feature details of  
 325 artistic images after different methods are applied. Eq. (17) presents how the SSIM is calculated:

$$326 \quad \text{SSIM} = \left( \frac{2 \times nQ_1 \times nQ_2 + C_1}{Q_1^2 + Q_2^2 + C_1} \times \frac{2 \times \zeta Q_1 \times \zeta Q_2 + C_2}{Q_1^2 + Q_2^2 + C_2} \times \frac{\zeta Q_1 Q_2 + C_3}{Q_1 Q_2 + C_3} \right)^\mu \quad (17)$$

327 where  $Q_1$  and  $Q_2$  represent the original image and the enhanced image respectively;  $nQ_1$

328 and  $nQ_2$  represent the means of pixels of  $Q_1$  and  $Q_2$  respectively;  $\zeta Q_1$  and  $\zeta Q_2$  represent the pixel

329 standard deviation of  $Q_1$  and  $Q_2$ , respectively;  $\zeta Q_1 Q_2$  represents the pixel covariance of  $Q_1$  and  $Q_2$ ;

330  $C_1$ ,  $C_2$ , and  $C_3$  represent constants, which are implemented to avoid cases where the denominator

331 is zero, and  $\mu$  is a constant in the range  $[0, 1]$ , which controls the importance of brightness to  
 332 structural similarity.

333 When the SSIM is calculated, the image is generally divided into a series of non-overlapping  
 334 small blocks, and the SSIM score of each small block is calculated. Then, the SSIM scores of all  
 335 small blocks are averaged to get the final SSIM score. The SSIM changes in  $[0, 1]$ . The closer the  
 336 value is to 1, the more similar the structure of the two images is and the better the quality is.

337 After applying different methods, the SSIM scores of artistic images are shown in Table 1.

338

339 Table 1 The statistical result of the SSIM score of artistic image

340

341 Table 1 depicts that as the time increases in the experiment, the SSIM of the artistic images

342 after feature enhancement processing also changes with the applications of different methods.

343 After the method in [5] is applied, the SSIM of the images changes between 0.862 to 0.896 and

344 reaches the maximum score in 50 tests. After the method in [6] is applied, the SSIM of images

345 ranges between 0.833-0.885 and reaches the maximum score at 40 tests. After the proposed method

346 is implemented, the SSIM of the images ranges between 0.936 to 0.973 and also reaches the

347 maximum score at 40 tests. Based on the above tests, after the proposed method is applied, the

348 SSIM of the image gets higher, indicating the enhancement processing effect of the proposed

349 method.

350 The average gradient can reflect the clarity of the image and the change of details after feature

351 enhancement is run. In general, the larger the average gradient, the more prominent the image

352 texture features and the better the detail retention effect. Eq. (18) presents how it is computed:

$$353 \quad \xi = \frac{\sum_{x=1}^X \sum_{y=1}^Y \sqrt{(f(x-1,y) - f(x,y))^2 + (f(x,y-1) - f(x,y))^2}}{(X+1)(Y+1)} \quad (18)$$

354

355 where  $f(x,y)$  represents the pixel value corresponding to the row  $x$  and column  $y$  of the  
356 image;  $f(x-1,y) - f(x,y)$  and  $f(x,y-1) - f(x,y)$  represents the first-order difference of  $f(x,y)$   
357 under  $x$  or  $y$ , respectively.

358 After applying different methods, the average gradient of artistic images is shown in Figure  
359 4.

360  
361 Figure 4 The statistical results of the mean gradient of the image.

362  
363 Figure 4 depicts that after the proposed method is implemented, the average gradient curve  
364 of the artistic image after feature enhancement processing is always higher than the average  
365 gradient curve of the two comparison methods and the original image, and the maximum score is  
366 close to 0.8, indicating that after the proposed method is implemented, The clarity of details in  
367 artistic images becomes much higher.

368  
369 4 Conclusion

370  
371 A new feature enhancement method for artistic images is designed based on histogram  
372 equalization and bilateral filtering. The proposed method is expressed as follows:

373 Firstly, the form of multi-stage processing is adopted to delimit the multi-stage enhancement  
374 processing level of the image by multi-band decomposition based on dividing the high and low-  
375 frequency representations of an artistic image. To fuse different scales of the image, the structure  
376 information and texture features of the image can be described better, which provides more  
377 powerful support for the subsequent feature enhancement processing. Secondly, the artistic image  
378 is denoised by bilateral filtering. Then, the histogram equalization method is employed to correct  
379 the gray level histogram of the image, so that the pixel intensity distribution of the image becomes  
380 more uniform and the contrast of the image is improved in the end. Finally, the features of the  
381 artistic image are enhanced by global tone mapping. The image is sharpened to highlight the  
382 feature edges and details to further improve the enhancement effect after histogram equalization  
383 processing is run.

384 Experimental results show that the proposed method is effective in improving the image  
385 quality. The image SSIM index becomes as high as 0.973, and the average gradient is close to 0.8.

386 The limitation of the research is based on a limited number of samples. More data-based  
387 investigations should be run and compared to get more reliable outcomes. Also, the variety of  
388 images should be increased

389 Future research will focus on more data samples and varied samples to derive more insights  
390 and better images

391  
392  
393 Appendix

394 *I have used the freely available images for experimentation of our model, which can be found*

395 at the following links [https://www.rawpixel.com/image/2421383/free-illustration-png-art-deco-](https://www.rawpixel.com/image/2421383/free-illustration-png-art-deco-seamless-pattern)  
396 [seamless-pattern](https://www.rawpixel.com/image/2421383/free-illustration-png-art-deco-seamless-pattern).

397  
398 [https://brightside.me/articles/an-artist-creates-visual-illusions-that-will-first-deceive-your-](https://brightside.me/articles/an-artist-creates-visual-illusions-that-will-first-deceive-your-eyes-then-take-over-your-heart-797089/?utm_source=brightside_web&utm_medium=article&utm_campaign=share_image&utm_content=copylink_797089&image=27279890#image27279890)  
399 [eyes-then-take-over-your-heart-](https://brightside.me/articles/an-artist-creates-visual-illusions-that-will-first-deceive-your-eyes-then-take-over-your-heart-797089/?utm_source=brightside_web&utm_medium=article&utm_campaign=share_image&utm_content=copylink_797089&image=27279890#image27279890)

400 [797089/?utm\\_source=brightside\\_web&utm\\_medium=article&utm\\_campaign=share\\_image&ut](https://brightside.me/articles/an-artist-creates-visual-illusions-that-will-first-deceive-your-eyes-then-take-over-your-heart-797089/?utm_source=brightside_web&utm_medium=article&utm_campaign=share_image&utm_content=copylink_797089&image=27279890#image27279890)  
401 [m\\_content=copylink\\_797089&image=27279890#image27279890](https://brightside.me/articles/an-artist-creates-visual-illusions-that-will-first-deceive-your-eyes-then-take-over-your-heart-797089/?utm_source=brightside_web&utm_medium=article&utm_campaign=share_image&utm_content=copylink_797089&image=27279890#image27279890).

## References

- [1] Zheng Huangyuying. Innovative design method of art images based on the integration of visual communication elements[J].Computer Informatization and Mechanical System, 2023, 6(3):71-75.
- [2] Guo Yong. Fuzzy line enhancement scheme of computer art image based on DRL algorithm[J].Journal of Computational Methods in Sciences and Engineering, 2023, 23(2):949-961.
- [3] Chen Tong, Yang Juan. Very deep fully convolutional encoder-decoder network based on wavelet transform for art image fusion in a cloud computing environment[J]. Evolving Systems, 2022, 14(2):281-293.
- [4] Kobayashi Taisuke, Kitaoka Akiyoshi, Kosaka Manabu, Tanaka Kenta, Watanabe Eiji. Motion illusion-like patterns extracted from photo and art images using predictive deep neural networks[J].Scientific Reports, 2022, 12(1):3893-3903.
- [5] Zhou Kai, Li Jing. A low illumination laser image feature enhancement method based on a convolutional network model[J].Laser Journal, 2023, 44(12):120-125.
- [6] Wand Dexing, YANG Yurui, YUAN Hongchun, GAO Kai. Underwater image enhancement method combining feature fusion and physical correction[J].Chinese Journal of Liquid Crystals and Displays, 2023, 38(11):1554-1566.
- [7] Liang Liming, ZHU Chenkun, HE Anjun. Multi-level Feature Fusion Algorithm for Low Illumination Image Enhancement[J].Radio Engineering, 2023, 53(04):946-956.
- [8] Li Rui Kang, Li MengHao, Chen ShiQi, Chen YueTing, Xu ZhiHai. Dark2Light: multi-stage progressive learning model for low-light image enhancement.[J]. Optics Express, 2023, 31(26):42887-42900.
- [9] Zhang Dehuan, Wu Chenyu, Zhou Jingchun, Zhang Weishi, Lin Zifan, Polat Kemal, Alenezi Fayadh. Robust underwater image enhancement with cascaded multi-level sub-networks and triple attention mechanism[J].Neural Networks, 2024, 169:685-697.
- [10] Seungchul Ryu, Hyunjin Yoo, Tara Akhavan. P-17: All Weather-Robust Image Quality Enhancement based on Image Feature Fusion and Multiscale Degradation Profile[J].SID Symposium Digest of Technical Papers, 2023, 54(1):1715-1718.
- [11] Kwon Ki Hoon, Erdenebat Munkh Uchral, Kim Nam, Kwon Ki Chul, Kim Min Young. Image quality enhancement of 4D light field microscopy via reference image propagation-based one-shot learning[J]. Applied Intelligence, 2023, 53(20):23834-23852.
- [12] Ding Xiaxu, Liu Yi, Yan Hongxu, Zhang Pengcheng, Guo Niu, Gui Zhiguo. Industrial X-ray image enhancement network based on a ray scattering model.[J]. Applied optics, 2023, 62(20):5526-5537.
- [13] Zeng Pingping. Image texture enhancement method based on convolutional neural network[J].Computer Informatization and Mechanical System, 2023, 6(2):17-21.
- [14] Liu Xu, Lin Sen, Tao Zhiyong. Learning multiscale pipeline gated fusion for underwater image enhancement[J].Multimedia Tools and Applications, 2023, 82(21):32281-32304.
- [15] Yang Shaoliang, Zhou Dongming. Single Image Low-Light Enhancement via a Dual-

- 444 Path Generative Adversarial Network[J].Circuits, Systems, and Signal Processing, 2023,  
445 42(7):4221-4237.
- 446 [16] Wu Yirui, Wu Benze, Zhang Yunfei, Wan Shaohua. A novel method of data and feature  
447 enhancement for few-shot image classification[J].Soft Computing, 2023, 27(8):5109-5117.
- 448 [17] Gong An, Li Zhonghao, Wang Heng, Li Guangtong. Attention-guided network with  
449 hierarchical global priors for low-light image enhancement[J].Signal, Image and Video  
450 Processing, 2022, 17(5):2083-2091.
- 451 [18] Liu Fangjin, Hua Zhen, Li Jinjiang, Fan Linwei. Dual UNet low-light image  
452 enhancement network based on attention mechanism[J].Multimedia Tools and Applications, 2022,  
453 82 (16):24707-24742.
- 454 [19] Wang Rong, Zhang Yonghui, Zhang Jian. An efficient swing transformer-based method  
455 for underwater image enhancement[J].Multimedia Tools and Applications, 2022, 82 (12):18691-  
456 18708.
- 457 [20] Xu Xintao, Li Jinjiang, Hua Zhen, Fan Linwei. Attention-based multi-channel feature  
458 fusion enhancement network to process low-light images[J].IET Image Processing, 2022,  
459 16(12):3374-3393.
- 460  
461  
462  
463  
464

# Figure 1

Artistic image multilevel enhancement processing hierarchy classification diagram

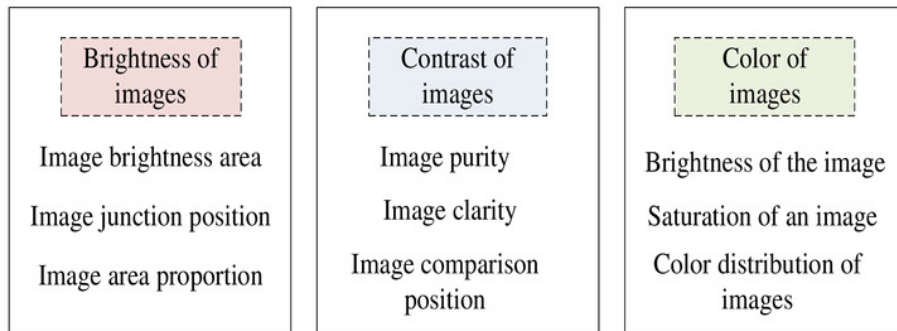


## Figure 2

Sample image

rawpixel, "Art nouveau wisteria flower pattern transparent png design resource



(a)



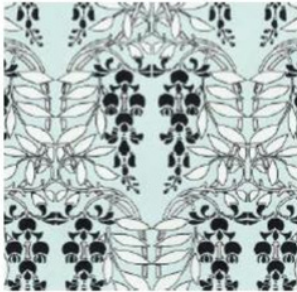
(b)

## Figure 3

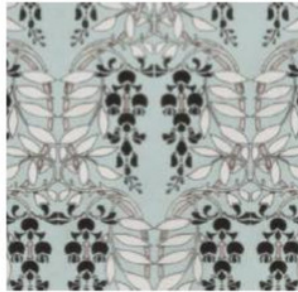
Feature enhancement processing results

rawpixel, "Art nouveau wisteria flower pattern transparent png design resource

Method of this paper



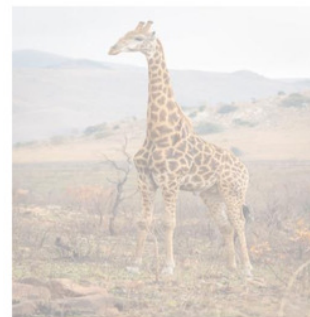
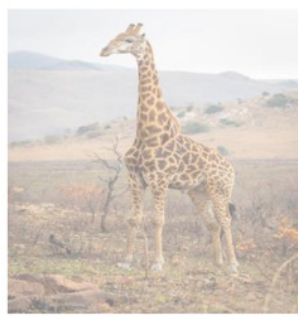
Method of reference [5]



Method of reference [6]



(a)



(b)

## Figure 4

Statistical results of image mean gradient

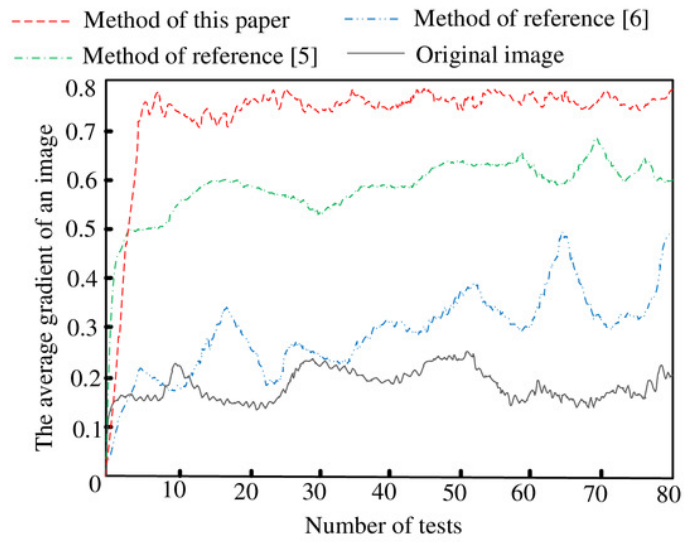


**Table 1** (on next page)

Statistical result of SSIM value of artistic image

| Number of tests | SSIM                 |                         |                         |
|-----------------|----------------------|-------------------------|-------------------------|
|                 | Method of this paper | Method of reference [5] | Method of reference [6] |
| 10              | 0.936                | 0.864                   | 0.835                   |
| 20              | 0.940                | 0.891                   | 0.858                   |
| 30              | 0.951                | 0.874                   | 0.869                   |
| 40              | 0.973                | 0.862                   | 0.885                   |
| 50              | 0.958                | 0.896                   | 0.833                   |

1